ORIGINAL ARTICLE

Cortical sensorimotor alterations classify clinical phenotype and putative genotype of spasmodic dysphonia

G. Battistella[a], S. Fuertinger[a], L. Fleysher[b], L. J. Ozelius[c] and K. Simonyan[a,d]

[a]*Department of Neurology, Icahn School of Medicine at Mount Sinai, New York, NY;* [b]*Department of Radiology, Icahn School of Medicine at Mount Sinai, New York, NY;* [c]*Department of Neurology, Massachusetts General Hospital, Charlestown, MA; and* [d]*Department of Otolaryngology, Icahn School of Medicine at Mount Sinai, New York, NY, USA*

Keywords:
dystonia, imaging marker, resting-state networks

Received 13 November 2015
Accepted 13 May 2016

European Journal of Neurology 2016, **23:** 1517–1527

doi:10.1111/ene.13067

Background and purpose: Spasmodic dysphonia (SD), or laryngeal dystonia, is a task-specific isolated focal dystonia of unknown causes and pathophysiology. Although functional and structural abnormalities have been described in this disorder, the influence of its different clinical phenotypes and genotypes remains scant, making it difficult to explain SD pathophysiology and to identify potential biomarkers.

Methods: We used a combination of independent component analysis and linear discriminant analysis of resting-state functional magnetic resonance imaging data to investigate brain organization in different SD phenotypes (abductor versus adductor type) and putative genotypes (familial versus sporadic cases) and to characterize neural markers for genotype/phenotype categorization.

Results: We found abnormal functional connectivity within sensorimotor and frontoparietal networks in patients with SD compared with healthy individuals as well as phenotype- and genotype-distinct alterations of these networks, involving primary somatosensory, premotor and parietal cortices. The linear discriminant analysis achieved 71% accuracy classifying SD and healthy individuals using connectivity measures in the left inferior parietal and sensorimotor cortices. When categorizing between different forms of SD, the combination of measures from the left inferior parietal, premotor and right sensorimotor cortices achieved 81% discriminatory power between familial and sporadic SD cases, whereas the combination of measures from the right superior parietal, primary somatosensory and premotor cortices led to 71% accuracy in the classification of adductor and abductor SD forms.

Conclusions: Our findings present the first effort to identify and categorize isolated focal dystonia based on its brain functional connectivity profile, which may have a potential impact on the future development of biomarkers for this rare disorder.

Introduction

Spasmodic dysphonia (SD), or laryngeal dystonia, is a task-specific focal dystonia affecting the laryngeal muscles predominantly during speaking but not during emotional vocalizations, such as laughing or crying. As with other forms of focal dystonia, the causes and pathophysiology of SD remain unclear, although its clinical symptoms are well defined [1,2]. Existing literature reports the presence of structural and functional abnormalities in the primary sensorimotor and secondary somatosensory cortices, basal ganglia, thalamus, and cerebellum [3–10], which appear to constitute the dystonic brain network [11] and also contribute to the control of sensorimotor aspects of speech production [12]. In addition, striatal

Correspondence: K. Simonyan, Department of Neurology, One Gustave L. Levy Place, Box 1137, Icahn School of Medicine at Mount Sinai, New York, NY 10029, USA (tel.: +1 212 241-0656; fax: +1 646 537-8628; e-mail: kristina.simonyan@mssm.edu).

EUROPEAN JOURNAL OF NEUROLOGY

dopaminergic function is altered in SD, characterized by decreased availability of D_2/D_3 receptors and abnormal release of endogenous dopamine during symptomatic and asymptomatic tasks [13]. However, despite the considerable progress made in mapping brain alterations in SD, our understanding of the interplay between disorder etiology and pathophysiology remains very limited. Specifically, it is unknown whether any of these reported brain abnormalities may be considered as a neuroimaging marker(s) for SD prediction and diagnostic differentiation. This is partly due to the fact that the majority of studies have focused on mapping brain alterations in the most common sporadic adductor form of SD, thus rendering it difficult to employ classifier algorithms for disorder characterization and the assessment of a more complete pathophysiological picture of this disorder across its different phenotypes and genotypes.

In a large cohort of patients with SD, we examined distinct patterns of abnormal functional connectivity and predictive imaging markers of disorder categorization between adductor (ADSD) and abductor (ABSD) forms of SD as well as between sporadic and familial cases as representatives of potentially different genotypes. We used multivariate classification algorithm of linear discriminant analysis (LDA) using the measures of between-group differences in resting-state functional connectivity derived from an independent component analysis (ICA). Resting-state networks are based on the measure of intrinsic low-frequency physiological fluctuations in the blood-oxygen-level-dependent signal and reflect the organization of both structural and task-related functional brain networks [14–16]. Patients with different forms of focal dystonia have been previously reported to exhibit altered resting-state connectivity [17–21].

Classification algorithms represent a powerful tool for identification of single traits or a combination of features that characterize and separate two or more classes of objects or subjects. Algorithmic classifiers have been successfully applied in several neurodegenerative disorders using structural [22,23] and functional [24–26] magnetic resonance imaging (fMRI) measures. Machine learning and fMRI voxel-wise multivariate classification were implemented as powerful tools for decoding neural representations of thoughts or physical objects at a particular time-point [27–29], with the LDA being validated in both normal [30–33] and disordered [34–37] states.

Based on previous studies in SD [3–10], we hypothesized that SD as a disorder can be distinguished from a normal state based on significant alterations within the sensorimotor network (SMN), whereas different SD forms can be categorized based on additional and combined abnormalities within the SMN and frontoparietal network (FPN). As SD is a task-specific disorder impairing a highly learned behavior, i.e. speech, we hypothesized that the predictive imaging markers for SD phenotype/genotype categorization would be found within cortical rather than subcortical regions.

Materials and methods

Study participants

We recruited 98 patients with SD, who were grouped based on their clinical phenotype (ADSD and ABSD) and underlying putative genotype (sporadic and familial SD). Among these, 15 patients were excluded due to excessive motion artifacts and incidental neuroradiological findings. The final groups consisted of 60 patients with sporadic SD (30 ABSD/30 ADSD) and 23 patients with familial SD (18 ADSD/5 ABSD) as well as 30 age- and gender-matched healthy volunteers (see demographic details in Table 1).

All participants were monolingual, native English speakers, and had normal scores on the Mini-Mental State Examination. With the exception of one patient with familial SD, all participants were right-handed as determined by the Edinburgh Handedness Inventory. None of the participants had a past or present history of any neurological (other than SD), psychiatric or laryngeal disorder. Diagnosis of SD was confirmed based on fiber-optic nasolaryngoscopy. All patients were fully symptomatic and had abstained from botulinum toxin injections for at least 3 months prior to the study.

All participants provided written informed consent, which was approved by the Internal Review Board at the Icahn School of Medicine at Mount Sinai.

Magnetic resonance imaging acquisition protocol

Whole-brain images were acquired on a Phillips 3T scanner equipped with an eight-channel head-coil. Resting-state fMRI data were obtained using a single-shot echo-planar imaging gradient echo sequence (repetition time, 2000 ms; echo time, 30 ms; flip angle, 90°; field of view, 240 mm; voxel size, 3×3 mm with 33 slices of 3.5 mm). A total of 150 volumes were acquired during a 5-min scan. Participants were instructed to keep their eyes closed without falling asleep or thinking of anything in particular during scanning. A sagittal T1-weighted gradient-echo sequence [Three-dimension (3D) magnetization-prepared rapid gradient-echo (MPRAGE); 172 contiguous slices; 1 mm^3 voxel; repetition time, 7.5 ms; echo time, 3.5 ms; field of view, 210 mm] was acquired for brain segmentation and functional image registration. Head movements during scanning were minimized by cushioning the

Table 1 Demographic characteristics and clinical data

	Sporadic		Familial		
	ADSD	ABSD	ADSD	ABSD	Controls
Number of subjects	30	30	18	5	30
Age (years) (mean ± SD)	55.4 ± 8.3	52.9 ± 12.7	56.3 ± 15.5	63.4 ± 5.8	49.7 ± 9.5
Gender (female/male)	23/7	26/4	16/2	2/3	18/12
Ethnicity (Caucasian/African-American/other	28/1/1	26/3/1	16/0/0	5/0/0	16/11/3
Handedness (Edinburgh Inventory)	Right				
Language	Monolingual native English				
Cognitive status	Mini-Mental State Examination ≥ 27 points				
Genetic status	Negative for DYT1, DYT6, DYT4 and DYT25				
Disease duration (years) (mean ± SD)	11.8 ± 9	15 ± 9.3	19.7 ± 13.9	19.2 ± 13.4	N/A
Age of onset (years) (mean ± SD)	43.6 ± 11.2	38 ± 12.7	36.6 ± 16.7	44.2 ± 12.9	N/A

ABSD and ADSD, adductor and abductor forms of spasmodic dysphonia.

participant's head in the coil; all subjects were monitored for any movements while in the scanner.

Data analysis

Preprocessing

Resting-state fMRI data were preprocessed using FSL and AFNI software. Following the removal of the first four volumes due to possible T1 stabilization effects, intra-session acquisitions were realigned to the fifth scan using a six-parameter rigid-body transformation and high-pass filtered with a cut-off frequency of 0.01 Hz (Gaussian-weighted least squares straight line fitting). Resultant images were then coregistered to the respective anatomical acquisition and normalized to the AFNI standard Talairach–Tournoux brain using a 12-parameter affine transformation with the follow-up optimization of normalization using a nonlinear algorithm in AFNI software. To control for possible motion and physiological noise effects, four-dimensional time-series in each subject were regressed using eight parameters, including white matter (WM) and cerebrospinal fluid (CSF) mean signal and six motion parameters calculated during realignment. WM and CSF covariates were extracted by automatically segmenting the MPRAGE into the gray matter, WM and CSF using the unified segmentation approach [38] in SPM8 software. WM and CSF maps were thresholded at 90% of tissue probability and applied to each time-series. All voxels in the masks were then averaged across all time-series to extract nuisance regressors. Final images were smoothed using a 5-mm Gaussian kernel full-width at half-maximum and mean-based intensity normalized as an input for group ICA analysis.

Feature selection

Multivariate classification methods consist of three main stages: (i) feature extraction; (ii) dimensionality reduction; and (iii) feature-based classification with cross-validation [39]. Feature selection was used to reduce the number of features and remove irrelevant and redundant data, thus improving classification performance. As input to the LDA, we used the features extracted from a multivariate ICA. For this, pre-processed time-series in all subjects were concatenated and decomposed into spatially independent components using a temporal concatenation approach [40] implemented in the MELODIC tool (Multivariate Exploratory Linear Optimized Decomposition into Independent Components) of FSL software. All obtained components were visually examined, and those that were spatially similar to previously identified networks [40,41] and had relevance to dystonia pathophysiology [17,19,20,42,43] were extracted for further between-group analysis using dual regression [31,44]. Voxel-based inferential statistics were computed using the individual Z-value maps of the dual regression. One-way ANOVA was used to assess the overall group differences between 30 healthy controls and 32 patients with SD, including 16 sporadic and 16 familial cases with a balanced representation of patients with ADSD and ABSD. To examine the effects of SD genotype and phenotype on resting-state connectivity profiles, we compared (i) 30 patients with sporadic SD and 23 patients with familial SD and (ii) 35 patients with ADSD (30 sporadic and 5 familial cases) and 35 patients with ABSD (30 sporadic and 5 familial cases), respectively. Statistical thresholds were set at a corrected family-wise error (FWE) of $P \leq 0.01$ to account for multiple comparisons. Significant clusters derived from between-group analyses were used in the subsequent classification analyses to identify the most informative brain region or the combination of regions that maximized the differentiation of patients with SD from healthy controls, patients with ADSD from patients with ABSD, and sporadic from familial SD cases.

Linear discriminant analysis

The mean signal of each significant cluster in between-group ICA comparisons was used as a feature of the LDA. To reduce the initial number of extracted features, we used a variable ranking procedure and a feed-forward selection procedure [39]. The first step ranked the features using the absolute value of the standardized *U*-statistic of a two-sample Wilcoxon test. This allowed the ranking of variables by optimizing the covariance matrix for subsequent feature classification based on the minimum number of significant features. The ordered variables were included as predictors in the LDA, starting from the highest rank and subsequently adding more features in the order of decreasing rank. Variable selection was stopped after the best discrimination power was achieved. The latter was defined as the percentage of correctly classified samples in a leave-one-out cross-validation procedure, i.e. an iterative removal of one subject from the dataset, construction of the predictor for the remaining data, and classification of the removed subject [39].

Results

The initial ICA analysis identified both shared and distinct patterns of abnormal resting-state functional connectivity within the SMN and FPN but not default-mode network across different phenotypes and genotypes of SD at an FWE-corrected $P \leq 0.01$.

The SMN is generally composed of functionally connected regions in the prefrontal cortex, premotor cortex and primary sensorimotor cortices as well as inferior and superior parietal cortices [16,45] (Fig. 1a).

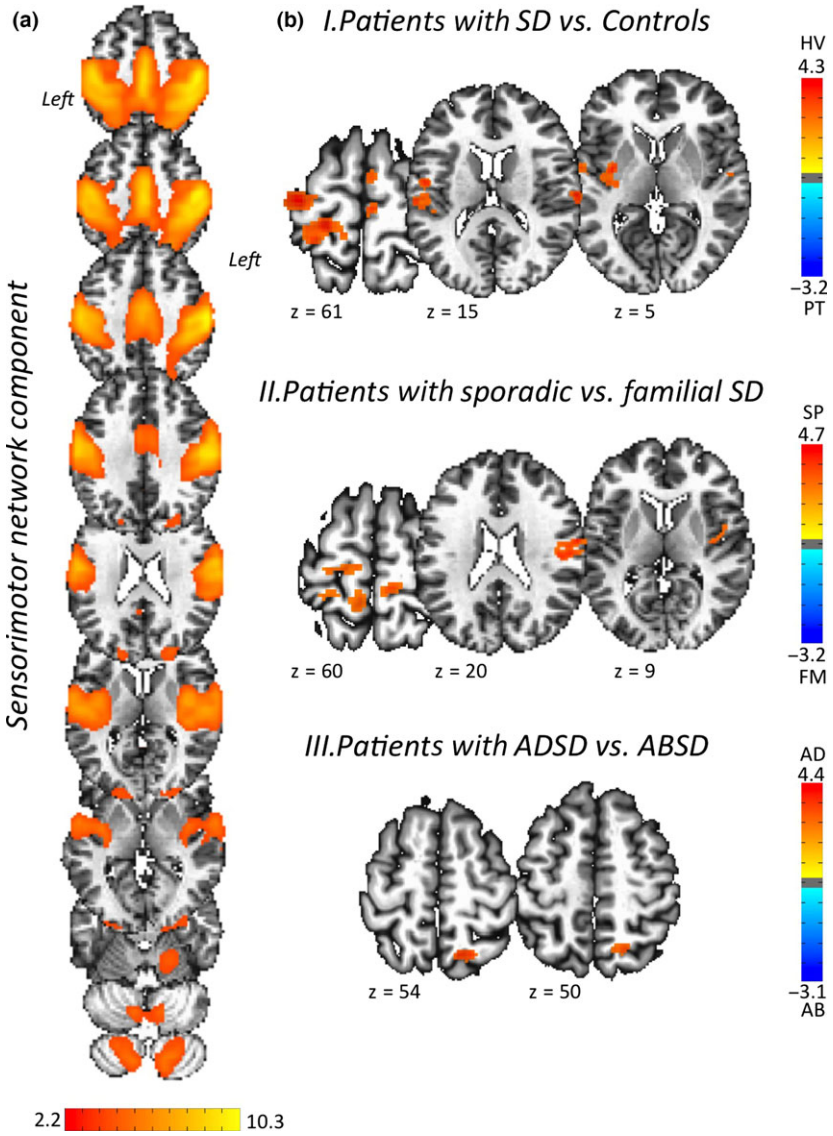

Figure 1 Sensorimotor functional network alteration assessed using independent component analysis. (a) Sensorimotor network extracted across all patients with spasmodic dysphonia (SD) and controls. Voxel-based inferential statistics were used to compare (b-I) all patients with SD versus healthy controls, (b-II) patients with sporadic versus familial SD, and (b-III) patients with adductor (ADSD) versus abductor (ABSD) forms of SD. Statistical maps are superimposed on a series of axial slices of the standard brain in Talairach–Tournoux space. The color bars represent *Z*-scores for independent components and *t*-scores for group statistical comparisons ($P \leq 0.01$, family-wise error-corrected). AB, patients with ABSD; AD, patients with ADSD; FM, patients with familial SD; HV, healthy control volunteers; PT, patients; SP, patients with sporadic SD.

Compared with healthy controls, all patients with SD showed decreased functional connectivity in the left sensorimotor cortex, inferior parietal cortex, putamen, right parietal operculum, and bilateral supplementary motor area (SMA) (Fig. 1b-I, Table 2). A direct comparison between sporadic and familial patients showed specific alterations of functional connectivity in the left sensorimotor cortex, right somatosensory cortex, SMA and insula as a potential influence of SD genotype (Fig. 1b-II, Table 2). A direct comparison between ADSD and ABSD groups found phenotype-specific differences in SMN connectivity in the right superior parietal cortex (Fig. 1b-III, Table 2).

The FPN is typically a left-lateralized spatial component that comprises extended regions of the parietal, inferior and middle frontal cortices, strongly corresponding to functional brain activity during cognitive and language processing [16,45] (Fig. 2a). Compared with healthy controls, all patients with SD showed increased functional connectivity in the left inferior parietal cortex (Fig. 2b-I, Table 2), with patients with familial SD exhibiting further abnormalities in this region compared with sporadic SD (Fig. 2b-II, Table 2). No significant clusters of distinctly abnormal FPN connectivity were identified in the direct comparison between patients with ADSD and ABSD.

The default mode network, one of the most widely studied resting-state networks, includes medial parietal regions (precuneus and posterior cingulate cortex) and ventromedial frontal cortex and is thought to characterize basic resting neural activity [16,45]. We did not find any significant differences in default mode network either between healthy controls and patients with SD or between the different SD subgroups.

Linear discriminant analysis

Patients with spasmodic dysphonia versus healthy controls

Based on data from the ICA analysis, the identified six clusters of functional connectivity alterations within the SMN and FPN (Table 2) were sorted by explanatory power for classification between disordered and normal states. The obtained rank (in decreasing order) included the left inferior parietal cortex, sensorimotor cortex, SMA, putamen, parietal operculum, and right superior temporal gyrus. Using the single, top-ranked cluster within the left inferior parietal cortex as a feature in the LDA, the accuracy of classification between patients with SD and healthy controls was 50% with 17 out of 32 patients and 14 out 30 controls being misclassified (Table 3). However, classification performance considerably improved when the LDA was based on the combination of the left inferior parietal and primary sensorimotor cortices, leading to a classification accuracy of 71%, with 9 out of 32 patients with SD and 9 out of 30 controls

Table 2 Peaks of activation of the significant clusters showing differences between the groups in the sensorimotor and frontoparietal network components

Brain cluster	Talairach coordinates at a cluster peak (x, y, z)			*t*-score
Sensorimotor network component				
Patients versus controls				
L sensorimotor cortex (areas 6, 4a, 1)	−22	−32	63	4.27
L supramarginal gyrus (area PFop)	−60	−26	23	4.3
L putamen	−30	−6	7	4.1
R supplementary motor area	2	−4	57	4.2
R parietal operculum/primary auditory cortex (area OP1/TE 1.0)	62	−18	15	3.7
Sporadic versus familial SD				
L sensorimotor cortex (areas 6, 4a, 3b)	−18	−22	65	4.7
R primary somatosensory cortex (area 3b)	58	−6	21	4.1
R supplementary motor area	6	−30	49	3.9
ADSD versus ABSD				
R superior parietal lobule (area 7A)	12	−60	53	3.8
R primary somatosensory cortex (areas 1, 2)	48	−34	51	2.94
R premotor cortex (area 6)	50	−10	49	3.29
Frontoparietal network component				
Patients versus controls				
L inferior parietal lobule (areas hIP1, hIP3)	−26	−42	37	3.8
Sporadic versus familial SD				
L inferior parietal lobule (hIP2)	−46	−40	43	4.2

ABSD and ADSD, adductor and abductor forms of spasmodic dysphonia (SD).

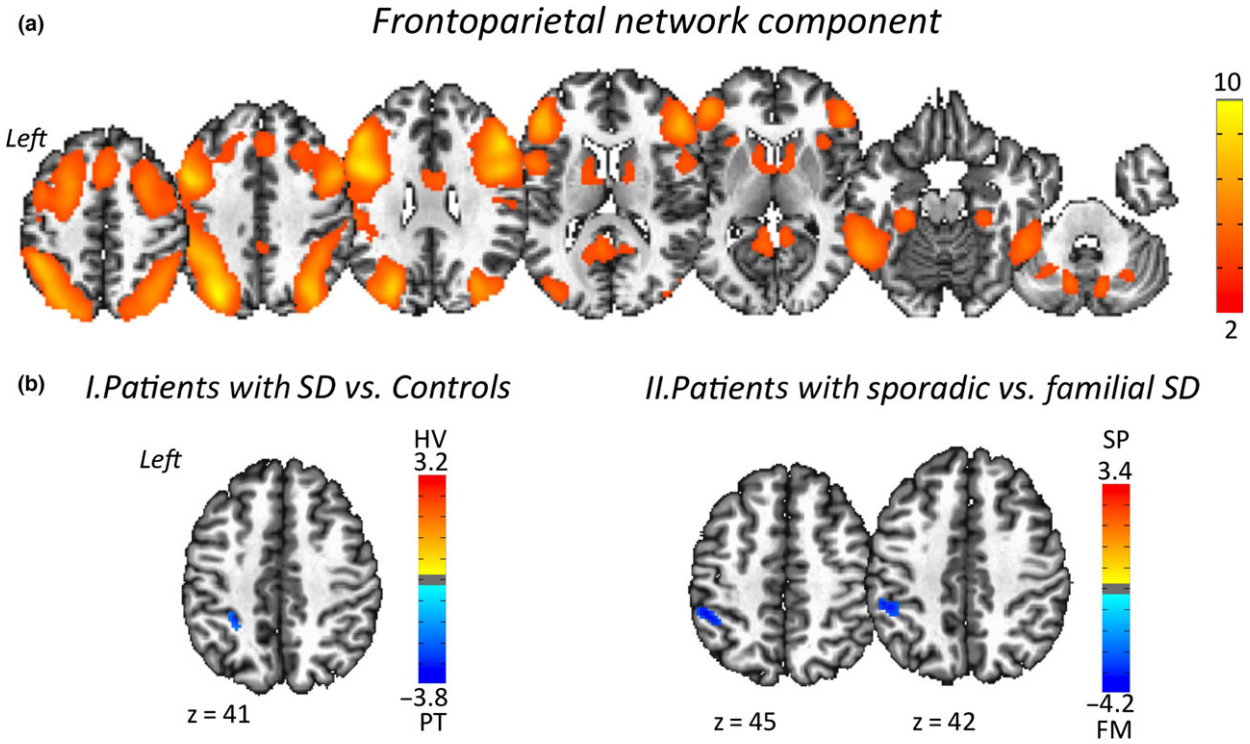

Figure 2 Frontoparietal functional network alteration assessed using independent component analysis. (a) Frontoparietal network extracted across all patients with spasmodic dysphonia (SD) and controls. Voxel-based inferential statistics were used to compare (b-I) all patients with SD versus healthy volunteers, and (b-II) patients with sporadic versus familial SD. Statistical maps are superimposed on a series of axial slices of the standard brain in Talairach–Tournoux space. The color bars represent *Z*-scores for independent components and *t*-scores for group statistical comparisons ($P \leq 0.01$, family-wise error-corrected). FM, patients with familial SD; HV, healthy control volunteers; PT, patients; SP, patients with sporadic SD.

Table 3 Performance of the linear discriminant analysis

		Misclassification rate	
Brain region	Accuracy rate	Patient with SD	Healthy control
Patients with SD versus healthy controls			
L inferior parietal lobule	50%	53% (17/32)	47% (14/30)
L inferior parietal lobule and L sensorimotor cortex	71%	28% (9/32)	30% (9/30)
Familial SD versus sporadic SD			
L inferior parietal lobule	68%	35% (8/23)	30% (9/30)
L inferior parietal lobule and R sensorimotor cortex and L premotor cortex	81%	13% (3/23)	23% (7/30)
ADSD versus ABSD			
R superior parietal lobule	65%	37% (13/35)	31% (11/35)
R superior parietal lobule and R primary somatosensory cortex and R premotor cortex	71%	34% (12/35)	23% (8/35)

ABSD and ADSD, adductor and abductor forms of spasmodic dysphonia (SD).

remaining misclassified (Fig. 3-I). Classification power did not improve by adding a third or more features (accuracy rate ≤ 64.5%).

Sporadic versus familial spasmodic dysphonia

Sorting the most explanatory features for SD putative genotype categorization between patients with sporadic and familial SD resulted in the following ranking of the four clusters of functional connectivity alterations (Table 2): the left inferior parietal cortex, right somatosensory cortex, left premotor cortex, and right SMA (in decreasing order). Using only the highest ranked feature in the LDA, i.e., the left inferior parietal cortex, the accuracy of classification between patients with sporadic and familial SD was 68%, with 8 out of 23 familial SD and 9 out of 30 sporadic SD

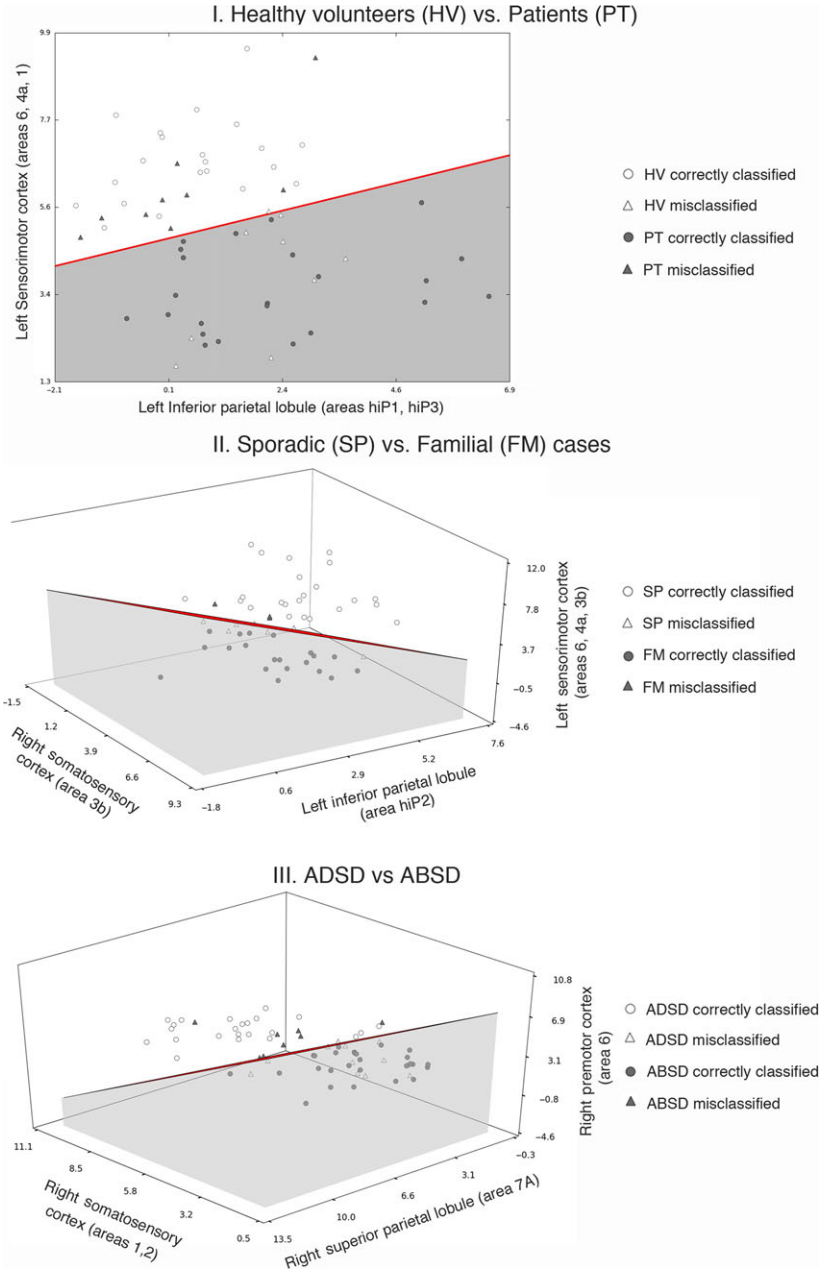

Figure 3 Results of the linear discriminant analysis of (I) patients with spasmodic dysphonia (SD) versus healthy volunteers, (II) patients with sporadic versus familial SD, and (III) patients with adductor (ADSD) versus abductor (ABSD) forms of SD. The scatter plots show the individual combinations of the mean values of the *Z*-score within (I) the left sensorimotor and the left inferior parietal cortices in patients (gray circles for correct classification and gray triangles for misclassification of patients) and healthy volunteers (empty circles for correct classification and empty triangles for misclassified healthy volunteers); (II) the left inferior parietal lobule, right somatosensory, and left sensorimotor cortices in sporadic SD (empty circles for correct classification and empty triangles for misclassification of sporadic patients) and familial SD (gray circles for correct classification and gray triangles for misclassification of familial patients); and (III) the right superior parietal lobule, somatosensory and premotor cortices in patients with ABSD (gray circles for correct classification and gray triangles for patients with misclassified ABSD) and patients with ADSD (empty circles for correct classification and empty triangles for misclassified ADSD). The red line (I) and red planes (II and III) represent the decision boundary of the classification. The corresponding values are provided in Table 3. FM, patients with familial SD; HV, healthy control volunteers; PT, patients; SP, patients with sporadic SD.

being misclassified. The best overall classification power of 81% accuracy between these two patient groups was obtained with the combination of left inferior parietal, premotor and right somatosensory cortices, with 3 out of 23 familial SD and 7 out of 30 sporadic SD being misclassified (Fig. 3-II, Table 3). The overall classification power did not improve by considering other combinations of the four brain regions (accuracy rate $\leq 81\%$).

Adductor versus abductor forms of spasmodic dysphonia

We identified only one region of significant functional alteration between patients with ADSD and ABSD, which was located in the right superior parietal cortex and yielded 65% accuracy (13 out of 35 ADSD and 11 out of 35 ABSD misclassified) of the LDA classifier when distinguishing between the two clinical phenotypes of SD (Table 3). As this accuracy rate was suboptimal, we lowered our statistical threshold from an FWE-corrected $P \leq 0.01$ to an FWE-corrected $P \leq 0.05$ in order to identify additional regions of abnormalities between these groups for a more comprehensive discriminative analysis. This strategy led to identification of further abnormalities in functional connectivity in the right primary somatosensory cortex and right premotor cortex between patients with

ADSD and ABSD. The classification power between patients with ADSD and ABSD based on the combination of the right superior parietal, primary somatosensory and premotor cortices increased to 71%, with 12 out of 35 ADSD and 8 out of 35 ABSD being misclassified (Fig. 3-III).

Discussion

Our study demonstrated that patients with SD exhibited functional connectivity alterations within the SMN and FPN, which varied in their extent between different clinical phenotypes (ADSD versus ABSD) and which might have been influenced by the involvement of different genetic factors in familial and sporadic cases. We further showed that abnormalities in the sensorimotor and parietal regions may serve as imaging markers for identification of SD as a disorder and its further classification into different subtypes (ADSD versus ABSD; sporadic versus familial SD). Specifically, combined alterations in the left inferior parietal and sensorimotor cortices permitted a reliable classification of patients with SD and healthy controls. A combination of abnormal functional connectivity measures in the right somatosensory cortex and left inferior parietal and premotor cortices showed high accuracy in distinguishing between sporadic and familial SD cases, whereas right-sided alterations in the superior parietal, primary somatosensory and premotor cortices defined distinct ADSD and ABSD phenotypes. As such, our study not only mapped functional network alterations in this disorder, but also used neuroimaging data to disambiguate SD from a normal state and differentiate the disorder based on its clinical and genetic heterogeneity, pointing to possible mechanistic aspects of SD pathophysiology.

Identification of spasmodic dysphonia as a disorder

Our overall findings showed greater impairment of the cortical network in SD, with major alterations identified in resting-state networks involved in the control of sensorimotor processing and motor planning (SMN) as well as multisensory integration and speech/language (FPN) [16,40]. Although the basal ganglia have been considered a key region in the pathophysiology of dystonia [46–48] and we did observe significantly reduced functional connectivity of the left putamen in this study, the greater involvement of cortical network abnormalities in SD pathophysiology and their combined accuracy in classifying this disorder may not be surprising. The extent of cortical network alterations may be explained by the fact that SD primarily affects speech production, which is a highly learned and skillful behavior, deeply relying on fine orchestration of multiple cortical networks [12,49,50]. Furthermore, the presence of predominantly left-sided network alterations may be reflected by the left-hemispheric dominance of speech-controlling networks in right-handed individuals, which appears to be affected in patients with SD. However, the left putamen, which we found to have decreased connectivity within the SMN, has been previously shown to exhibit reduced functional activity during symptomatic but not asymptomatic voice production [5], increased gray matter volume [6], and decreased D_2/D_3 receptor availability and endogenous dopamine release in patients with SD [13]. Although our present findings do not refute the notion that the putamen is involved in the pathophysiology of dystonia, it appears that functional alterations in this region may not provide sufficient discriminative information for accurate SD classification.

Contrary to some earlier studies in other forms of focal dystonia [19,20,42], we did not observe any significant alterations of the default-mode network in patients with SD. This discrepancy might be due to SD-specific brain organization, which is probably characterized by intrinsic networks controlling complex sensorimotor and executive tasks rather than the absence of specific goal-directed behaviors.

In comparison with healthy individuals, all patients with SD showed significant decreases in functional connectivity of the left primary sensorimotor/premotor cortex, putamen, inferior parietal lobule, bilateral SMA, as well as right parietal operculum and primary auditory cortex. Using these significant network abnormalities for the identification of the disordered state, we found that the combination of alterations in the left sensorimotor cortex and inferior parietal lobule provide 71% accuracy in classifying SD and healthy individuals. Functional and structural MRI studies as well as the assessments of cortical excitability with transcranial magnetic stimulation have previously reported alterations in sensorimotor regions in SD [3–6,9,51,52] and other forms of dystonia [53,54], pointing to their role in dystonia pathophysiology. Modulation of abnormal laryngeal and cortical sensorimotor activity following the treatment with botulinum toxin injections has also been hypothesized to be relevant to SD pathophysiology [3,55], although the literature in this domain remains somewhat scant and inconsistent [3,4]. Being well integrated in the sensorimotor interface [56–60], reduced activation of the parietal cortex in patients with dystonia has been associated with impaired processing of sensory information and abnormal coupling between sensory input and motor output [42,61], as well as abnormal

proprioceptive input via cerebellar connections [62,63]. Our current findings support a major role of the parietal cortex in the pathophysiology of dystonia in general and SD in particular and further highlight the importance of the left inferior parietal cortex (together with the left sensorimotor cortex) as a neuroimaging marker for SD discrimination from a normal state.

Identification of spasmodic dysphonia based on phenotype and genotype

Even though causative genes of SD have not yet been identified, cumulative evidence suggests that genetic susceptibility factors or dominantly inherited genes with reduced penetrance may be involved in SD genetic pathophysiology [64–66]. Our current findings of additional alterations of both SMN and FPN in familial versus sporadic SD cases suggest a possible effect of these genetic risk factors (albeit unknown) on functional connectivity alterations in familial versus sporadic SD. However, we found that the influence of SD phenotype was limited to distinct alterations within the SMN only, suggesting that dystonia phenotype may be provoked by differences in processing and execution of specific motor commands in patients with ABSD versus patients with ADSD. Furthermore, strictly right-lateralized abnormalities between patients with ABSD and ADSD may suggest possibly abnormal functional integration of both hemispheres in this disorder. Taken together, the presence of distinct alterations in functional connectivity between different forms of SD suggests the influence of phenotypic and genotypic characteristics on brain organization and sheds light on divergent, multifactorial pathophysiological pathways underlying distinct phenotype- and genotype-specific relationships in this disorder.

In conclusion, we found that, among all regions with reduced connectivity, the parietal cortex was one of the strongest regions that reliably discriminated between different SD clinical phenotypes and putative genotypes. Its discriminatory power was aided by addition of the sensorimotor cortex, which further underscores the parietal cortex as a possible imaging marker for identification and categorization of SD. As a fairly simple setup and a short acquisition time of resting-state fMRI datasets make their translation from a research methodology to clinical neuroradiology feasible, the results of our study provide a scientific foundation for further tests of more complex classification algorithms in larger patient cohorts with the ultimate goal of translating and implementing the current findings in clinical practice as well as helping to stratify patients for future studies involving gene discovery and clinical trials.

Acknowledgements

We thank Estee Rubien-Thomas, BA, and Heather Alexander, BA, for patient recruitment and imaging data acquisition. We thank Andrew Blitzer, MD, DDS, and Steven Frucht, MD, for patient referrals. This work was supported by R01DC01805 grant to K.S. from the National Institute on Deafness and Other Communication Disorders, National Institutes of Health.

Disclosure of conflicts of interest

G. Battistella, S. Fuertinger, and L. Fleysher declare no financial or other conflicts of interest .L. J. Ozelius serves on the Scientific Advisory Boards of the Benign Essential Blepharospasm Research Foundation, National Spasmodic Dysphonia Association, National Tourette's Syndrome Association and Cure AHC; she receives royalties from Athena Diagnostics. K. Simonyan serves on the Medical and Scientific Advisory Council of the Dystonia Medical Research Foundation.

References

1. Blitzer A. Spasmodic dysphonia and botulinum toxin: experience from the largest treatment series. *Eur J Neurol* 2010; **17**(Suppl. 1)**:** 28–30.
2. Brin MF, Blitzer A, Stewart C. Laryngeal dystonia (spasmodic dysphonia): observations of 901 patients and treatment with botulinum toxin. *Adv Neurol* 1998; **78:** 237–252.
3. Ali SO, Thomassen M, Schulz GM, *et al*. Alterations in CNS activity induced by botulinum toxin treatment in spasmodic dysphonia: an H215O PET study. *J Speech Lang Hear Res* 2006; **49:** 1127–1146.
4. Haslinger B, Erhard P, Dresel C, Castrop F, Roettinger M, Ceballos-Baumann AO. "Silent event-related" fMRI reveals reduced sensorimotor activation in laryngeal dystonia. *Neurology* 2005; **65:** 1562–1569.
5. Simonyan K, Ludlow CL. Abnormal activation of the primary somatosensory cortex in spasmodic dysphonia: an fMRI study. *Cereb Cortex* 2010; **20:** 2749–2759.
6. Simonyan K, Ludlow CL. Abnormal structure-function relationship in spasmodic dysphonia. *Cereb Cortex* 2012; **22:** 417–425.
7. Simonyan K, Tovar-Moll F, Ostuni J, *et al*. Focal white matter changes in spasmodic dysphonia: a combined diffusion tensor imaging and neuropathological study. *Brain* 2008; **131:** 447–459.
8. Samargia S, Schmidt R, Kimberley TJ. Cortical silent period reveals differences between adductor spasmodic dysphonia and muscle tension dysphonia. *Neurorehabil Neural Repair* 2016; **30:** 221–232.
9. Suppa A, Marsili L, Giovannelli F, *et al*. Abnormal motor cortex excitability during linguistic tasks in adductor-type spasmodic dysphonia. *Eur J Neurosci* 2015; **42:** 2051–2060.

10. Kostic VS, Agosta F, Sarro L, *et al*. Brain structural changes in spasmodic dysphonia: a multimodal magnetic resonance imaging study. *Parkinsonism Relat Disord* 2016; **25:** 78–84.
11. Lehericy S, Tijssen MA, Vidailhet M, Kaji R, Meunier S. The anatomical basis of dystonia: current view using neuroimaging. *Mov Disord* 2013; **28:** 944–957.
12. Fuertinger S, Horwitz B, Simonyan K. The functional connectome of speech control. *PLoS Biol* 2015; **13:** e1002209.
13. Simonyan K, Berman BD, Herscovitch P, Hallett M. Abnormal striatal dopaminergic neurotransmission during rest and task production in spasmodic dysphonia. *J Neurosci* 2013; **33:** 14705–14714.
14. Biswal B, Yetkin FZ, Haughton VM, Hyde JS. Functional connectivity in the motor cortex of resting human brain using echo-planar MRI. *Magn Reson Med* 1995; **34:** 537–541.
15. Damoiseaux JS, Greicius MD. Greater than the sum of its parts: a review of studies combining structural connectivity and resting-state functional connectivity. *Brain Struct Funct* 2009; **213:** 525–533.
16. Smith SM, Fox PT, Miller KL, *et al*. Correspondence of the brain's functional architecture during activation and rest. *Proc Natl Acad Sci USA* 2009; **106:** 13040–13045.
17. Dresel C, Li Y, Wilzeck V, Castrop F, Zimmer C, Haslinger B. Multiple changes of functional connectivity between sensorimotor areas in focal hand dystonia. *J Neurol Neurosurg Psychiatry* 2014; **85:** 1245–1252.
18. Delnooz CC, Pasman JW, Beckmann CF, van de Warrenburg BP. Altered striatal and pallidal connectivity in cervical dystonia. *Brain Struct Funct* 2015; **220:** 513–523.
19. Zhou B, Wang J, Huang Y, Yang Y, Gong Q, Zhou D. A resting state functional magnetic resonance imaging study of patients with benign essential blepharospasm. *J Neuroophthalmol* 2013; **33:** 235–240.
20. Mohammadi B, Kollewe K, Samii A, Beckmann CF, Dengler R, Munte TF. Changes in resting-state brain networks in writer's cramp. *Hum Brain Mapp* 2012; **33:** 840–848.
21. Termsarasab P, Ramdhani RA, Battistella G, *et al*. Neural correlates of abnormal sensory discrimination in laryngeal dystonia. *Neuroimage Clin* 2015; **10:** 18–26.
22. Fornari E, Maeder P, Meuli R, Ghika J, Knyazeva MG. Demyelination of superficial white matter in early Alzheimer's disease: a magnetization transfer imaging study. *Neurobiol Aging* 2012; **33:** e427–419.
23. Janousova E, Schwarz D, Kasparek T. Combining various types of classifiers and features extracted from magnetic resonance imaging data in schizophrenia recognition. *Psychiatry Res* 2015; **232:** 237–249.
24. Yourganov G, Schmah T, Churchill NW, Berman MG, Grady CL, Strother SC. Pattern classification of fMRI data: applications for analysis of spatially distributed cortical networks. *NeuroImage* 2014; **96:** 117–132.
25. Yun HJ, Kwak K, Lee JM. Alzheimer's disease neuroimaging. I. Multimodal discrimination of Alzheimer's disease based on regional cortical atrophy and hypometabolism. *PLoS One* 2015; **10:** e0129250.
26. Zhang D, Liu X, Chen J, Liu B. Distinguishing patients with Parkinson's disease subtypes from normal controls based on functional network regional efficiencies. *PLoS One* 2014; **9:** e115131.
27. Bauer AJ, Just MA. Monitoring the growth of the neural representations of new animal concepts. *Hum Brain Mapp* 2015; **36:** 3213–3226.
28. Just MA, Cherkassky VL, Buchweitz A, Keller TA, Mitchell TM. Identifying autism from neural representations of social interactions: neurocognitive markers of autism. *PLoS One* 2014; **9:** e113879.
29. Mason RA, Just MA. Physics instruction induces changes in neural knowledge representation during successive stages of learning. *NeuroImage* 2015; **111:** 36–48.
30. Hale JR, Mayhew SD, Mullinger KJ, *et al*. Comparison of functional thalamic segmentation from seed-based analysis and ICA. *NeuroImage* 2015; **114:** 448–465.
31. Leech R, Kamourieh S, Beckmann CF, Sharp DJ. Fractionating the default mode network: distinct contributions of the ventral and dorsal posterior cingulate cortex to cognitive control. *J Neurosci* 2011; **31:** 3217–3224.
32. Sami S, Robertson EM, Miall RC. The time course of task-specific memory consolidation effects in resting state networks. *J Neurosci* 2014; **34:** 3982–3992.
33. Smith DV, Utevsky AV, Bland AR, *et al*. Characterizing individual differences in functional connectivity using dual-regression and seed-based approaches. *NeuroImage* 2014; **95:** 1–12.
34. Kaufmann T, Skatun KC, Alnaes D, *et al*. Disintegration of sensorimotor brain networks in schizophrenia. *Schizophr Bull* 2015; **41:** 1326–1335.
35. Nugent AC, Robinson SE, Coppola R, Furey ML, Zarate CA Jr. Group differences in MEG-ICA derived resting state networks: application to major depressive disorder. *NeuroImage* 2015; **118:** 1–12.
36. Argyelan M, Gallego JA, Robinson DG, *et al*. Abnormal resting state FMRI activity predicts processing speed deficits in first-episode psychosis. *Neuropsychopharmacology* 2015; **40:** 1631–1639.
37. Tinaz S, Lauro P, Hallett M, Horovitz SG. Deficits in task-set maintenance and execution networks in Parkinson's disease. *Brain Struct Funct* 2016; **221:** 1413–1425.
38. Ashburner J, Friston KJ. Unified segmentation. *NeuroImage* 2005; **26:** 839–851.
39. Bishop CM. *Pattern Recognition and Machine Learning*. New York: Springer, 2006.
40. Beckmann CF, Smith SM. Probabilistic independent component analysis for functional magnetic resonance imaging. *IEEE Trans Med Imaging* 2004; **23:** 137–152.
41. van den Heuvel MP, Hulshoff Pol HE. Exploring the brain network: a review on resting-state fMRI functional connectivity. *Eur Neuropsychopharmacol* 2010; **20:** 519–534.
42. Delnooz CC, Helmich RC, Toni I, van de Warrenburg BP. Reduced parietal connectivity with a premotor writing area in writer's cramp. *Mov Disord* 2012; **27:** 1425–1431.
43. Hinkley LB, Sekihara K, Owen JP, Westlake KP, Byl NN, Nagarajan SS. Complex-value coherence mapping reveals novel abnormal resting-state functional connectivity networks in task-specific focal hand dystonia. *Front Neurol* 2013; **4:** 149.
44. Filippini N, MacIntosh BJ, Hough MG, *et al*. Distinct patterns of brain activity in young carriers of the APOE-epsilon4 allele. *Proc Natl Acad Sci USA* 2009; **106:** 7209–7214.
45. Beckmann CF, DeLuca M, Devlin JT, Smith SM. Investigations into resting-state connectivity using

independent component analysis. *Philos Trans R Soc Lond B Biol Sci* 2005; **360:** 1001–1013.
46. Berardelli A, Rothwell JC, Day BL, Marsden CD. Pathophysiology of blepharospasm and oromandibular dystonia. *Brain* 1985; **108:** 593–608.
47. Marsden CD. Motor disorders in basal ganglia disease. *Hum Neurobiol* 1984; **2:** 245–250.
48. Burton K, Farrell K, Li D, Calne DB. Lesions of the putamen and dystonia: CT and magnetic resonance imaging. *Neurology* 1984; **34:** 962–965.
49. Simonyan K, Fuertinger S. Speech networks at rest and in action: interactions between functional brain networks controlling speech production. *J Neurophysiol* 2015; **113:** 2967–2978.
50. Hickok G, Poeppel D. The cortical organization of speech processing. *Nat Rev Neurosci* 2007; **8:** 393–402.
51. Samargia S, Schmidt R, Kimberley TJ. Shortened cortical silent period in adductor spasmodic dysphonia: evidence for widespread cortical excitability. *Neurosci Lett* 2014; **560:** 12–15.
52. Samargia S, Schmidt R, Kimberley TJ. Cortical silent period reveals differences between adductor spasmodic dysphonia and muscle tension dysphonia. *Neurorehabil Neural Repair* 2016; **30:** 221–232.
53. Neychev VK, Gross RE, Lehericy S, Hess EJ, Jinnah HA. The functional neuroanatomy of dystonia. *Neurobiol Dis* 2011; **42:** 185–201.
54. Zoons E, Booij J, Nederveen AJ, Dijk JM, Tijssen MA. Structural, functional and molecular imaging of the brain in primary focal dystonia–a review. *NeuroImage* 2011; **56:** 1011–1020.
55. Bielamowicz S, Ludlow CL. Effects of botulinum toxin on pathophysiology in spasmodic dysphonia. *Ann Otol Rhinol Laryngol* 2000; **109:** 194–203.
56. Brownsett SL, Wise RJ. The contribution of the parietal lobes to speaking and writing. *Cereb Cortex* 2010; **20:** 517–523.
57. Culham JC, Valyear KF. Human parietal cortex in action. *Curr Opin Neurobiol* 2006; **16:** 205–212.
58. Shum M, Shiller DM, Baum SR, Gracco VL. Sensorimotor integration for speech motor learning involves the inferior parietal cortex. *Eur J Neurosci* 2011; **34:** 1817–1822.
59. Sereno MI, Huang RS. Multisensory maps in parietal cortex. *Curr Opin Neurobiol* 2014; **24:** 39–46.
60. Gottlieb J. From thought to action: the parietal cortex as a bridge between perception, action, and cognition. *Neuron* 2007; **53:** 9–16.
61. de Vries PM, Johnson KA, de Jong BM, *et al*. Changed patterns of cerebral activation related to clinically normal hand movement in cervical dystonia. *Clin Neurol Neurosurg* 2008; **110:** 120–128.
62. Fiorio M, Weise D, Onal-Hartmann C, Zeller D, Tinazzi M, Classen J. Impairment of the rubber hand illusion in focal hand dystonia. *Brain* 2011; **134:** 1428–1437.
63. Hagura N, Oouchida Y, Aramaki Y, *et al*. Visuokinesthetic perception of hand movement is mediated by cerebro-cerebellar interaction between the left cerebellum and right parietal cortex. *Cereb Cortex* 2009; **19:** 176–186.
64. Fuchs T, Saunders-Pullman R, Masuho I, *et al*. Mutations in GNAL cause primary torsion dystonia. *Nat Genet* 2013; **45:** 88–92.
65. Ozelius LJ, Lubarr N, Bressman SB. Milestones in dystonia. *Mov Disord* 2011; **26:** 1106–1126.
66. Parker N. Hereditary whispering dysphonia. *J Neurol Neurosurg Psychiatry* 1985; **48:** 218–224.